Journal of Colloid and Interface Science 646 (2023) 775–783

Contents lists available at ScienceDirect

Journal of Colloid And Interface Science

journal homepage: www.elsevier.com/locate/jcis

Contribution of non-ionic interactions on bile salt sequestration by chitooligosaccharides: Potential hypocholesterolemic activity

Filipe Coreta-Gomes [a,b,*], Inês M.V. Silva [a,b], Cláudia Nunes [c], Ildefonso Marin-Montesinos [d], Dmitry Evtuguin [d], Carlos F.G.C. Geraldes [b,e], Maria João Moreno [b], Manuel A. Coimbra [a]

[a] LAQV-REQUIMTE, Chemistry Department, University of Aveiro, 3810-193 Aveiro, Portugal
[b] Coimbra Chemistry Center – Institute of Molecular Sciences (CQC-IMS), Department of Chemistry, University of Coimbra, 3004-535 Coimbra, Portugal
[c] CICECO-Aveiro Institute of Materials, Department of Materials and Ceramic Engineering, University of Aveiro, 3810-193 Aveiro, Portugal
[d] CICECO-Aveiro Institute of Materials, Department of Chemistry, University of Aveiro, 3810-193 Aveiro, Portugal
[e] Department of Life Sciences, Faculty of Science and Technology, University of Coimbra, Calçada Martim de Freitas, 3000-393 Coimbra, Portugal

GRAPHICAL ABSTRACT

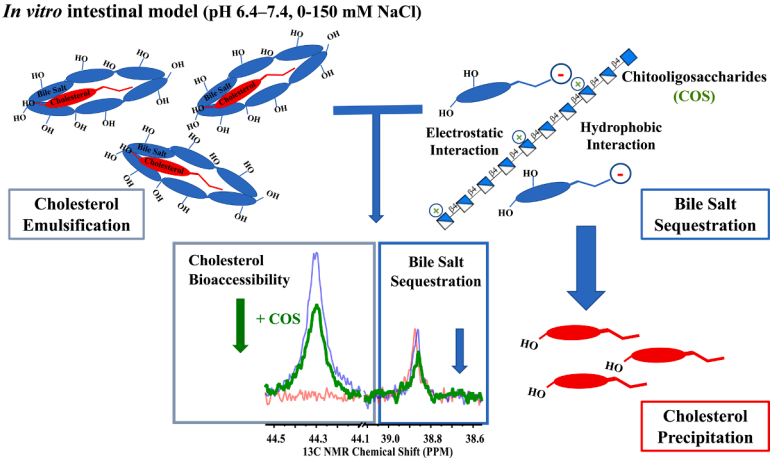

ARTICLE INFO

Keywords:
Chitooligosaccharides
Cholesterol bioaccessibility
Bile salts sequestration
Hypocholesterolemic ingredients

ABSTRACT

Chitooligosaccharides have been suggested as cholesterol reducing ingredients mostly due to their ability to sequestrate bile salts. The nature of the chitooligosaccharides-bile salts binding is usually linked with the ionic interaction. However, at physiological intestinal pH range (6.4 to 7.4) and considering chitooligosaccharides pKa, they should be mostly uncharged. This highlights that other type of interaction might be of relevance. In this work, aqueous solutions of chitooligosaccharides with an average degree of polymerization of 10 and 90 % deacetylated, were characterized regarding their effect on bile salt sequestration and cholesterol accessibility. Chitooligosaccharides were shown to bind bile salts to a similar extent as the cationic resin colestipol, both

* Corresponding author at: Chemistry Department, University of Aveiro, 3810-193 Aveiro, Portugal.
E-mail addresses: filipecoreta@ua.pt (F. Coreta-Gomes), imvs@qui.uc.pt (I.M.V. Silva), claudianunes@ua.pt (C. Nunes), imarin@ua.pt (I. Marin-Montesinos), dmitrye@ua.pt (D. Evtuguin), geraldes@ci.uc.pt (C.F.G.C. Geraldes), mmoreno@ci.uc.pt (M. João Moreno), mac@ua.pt (M.A. Coimbra).

https://doi.org/10.1016/j.jcis.2023.05.056
Received 21 November 2022; Received in revised form 24 April 2023; Accepted 8 May 2023
Available online 13 May 2023

decreasing cholesterol accessibility as measured by NMR at pH 7.4. A decrease in the ionic strength leads to an increase in the binding capacity of chitooligosaccharides, in agreement with the involvement of ionic interactions. However, when the pH is decreased to 6.4, the increase in charge of chitooligosaccharides is not followed by a significant increase in bile salt sequestration. This corroborates the involvement of non-ionic interactions, which was further supported by NMR chemical shift analysis and by the negative electrophoretic mobility attained for the bile salt-chitooligosaccharide aggregates at high bile salt concentrations. These results highlight that chitooligosaccharides non-ionic character is a relevant structural feature to aid in the development of hypocholesterolemic ingredients.

1. Introduction

Bile salts (BS) are biological detergents with amphiphilic nature, having a hydrophilic and a hydrophobic surface, and are negatively charged at physiological pH [1,2]. The most prevalent BS in the intestinal lumen are the ones conjugated with glycine. Their concentration in bile can go up to 50 mM [2]. There are two types of BS, the so-called primary BS which are synthesized by liver (such as glycochenodeoxycholic and glycocholic acids), and the secondary BS, resulting from microbiota biotransformation (such as glycodeoxycholic acid) [3-5]. Depending on their hydrophobic/hydrophilic balance, BS have different cholesterol solubility indexes, with glycodeoxycholic acid (GDCA) being the one with highest solubilizing capacity [6]. The cholesterol present in intestinal lumen may have origin exogenously, through the diet, or endogenously, produced by the liver and discharged from gallbladder after the major meals. BS are crucial for cholesterol absorption from both sources due to their ability to solubilize cholesterol [4,7,8]. Using an intestinal simplified model, it was shown that the solubilizing capacity for cholesterol is affected by the presence of polysaccharides such as arabinogalactans and galactomannans extracted from coffee [9], and laminarans and fucoidans from algae [10]. This effect was shown to be due to the sequestration of BS, [9] mostly by non-ionic interactions between BS and the polysaccharides. The decrease of cholesterol accessibility promoted by the polysaccharides is a determinant step on the permeation of sterols through the intestinal epithelium, as shown recently using Caco-2 cell monolayers [11]. Therefore, *in vitro* cholesterol accessibility assays are a suitable approach to characterize polysaccharides hypocholesterolemic potential, particularly regarding sequestration of BS mechanisms and cholesterol emulsification, since these events occur prior to the absorption of cholesterol into the blood. The formation of helical arrangements of BS molecules with oppositely charged polyelectrolytes of homopolymers or block copolymers have been shown, being considered promising candidates as BS sequestrants [12,13]. Positively charged polysaccharides such as chitosan and their oligosaccharides are also known to have BS sequestration ability, which is usually attributed to the electrostatic interaction between the positively charged (β1→4)-linked D-glucosamine groups of chitosan with the negatively charged BS [5]. Calorimetric studies have shown efficient interaction between chitosan and taurocholate acid at pH 3 [14]. However, as chitosan pKa varies from 6.2 to 6.5, modulated by molecular weight and degree of deacetylation [15,16], at physiological pH its low degree of protonation may not explain the observed *in vivo* hypocholesterolemic effect and higher excretion of BS [17,18]. This highlights that other structural characteristics beside positive charge can affect the interaction of BS with chitosan, namely the contribution of hydrophobic interactions. Higher degree of deacetylation and higher molecular weight are reported to promote chitosan hypocholesterolemic properties by mechanisms that include electrostatic interaction, adsorption, and entrapment due to the higher viscosity in intestinal lumen [19]. Chitosan low solubility at physiological pH and its high viscosity are technological limitations for their use has hypocholesterolemic agents, which have been overcome by strategies, such as enzymatic and partial acid hydrolysis to depolymerize them into chitooligosaccharides (COS). COS were shown to have a different BS binding capacity than chitosan, being dependent on the BS nature. Both of them have shown lower BS binding capacity than cationic resin cholestyramine [20]. Indeed, cationic resins, such as cholestyramine or colestipol, are currently used to treat hypercholesterolemic diseases. This pharmacological approach leads to the decrease of cholesterol blood levels by BS sequestration at intestinal lumen mainly due to electrostatic interactions. For this reason, these cationic resins based drugs have been shown to be a good model to evaluate, both *in vitro* and *in vivo*, the efficiency of BS sequestration [21-23]. To better clarify the hypocholesterolemic properties of COS and get insight on their mechanism of action focusing on cholesterol accessibility, in this work the interaction of a chitooligosaccharide with the BS GDCA was followed by zeta potential measurements and NMR.

2. Materials and Methods

2.1. Materials

Water-soluble commercial chitosan (Chitooligosaccharide) with 90 % deacetylation was bought to Carbosynth. Bile salt glycodeoxycholic acid (GDCA), Trizma® hydrochloride buffer (Tris), [4-^{13}C]Cholesterol, 3-(Trimethylsilyl)propionic-2,2,3,3-d_4 acid sodium salt (TSP), sodium nitrate ($NaNO_3$), 2-deoxyglucose, deuterated water (D_2O), methanol (MeOH), sodium azide (NaN_3), sodium chloride (NaCl), Dichloromethane, Chloroform ($CHCl_3$), Trifluoroacetic acid (TFA), Hydrochloric acid (HCl), Glacial acetic acid, Ammonia (NH_3) and Sodium borohydride ($NaBH_4$) were purchased to Sigma. The cationic resin Colestipol hydrochloride used was a USP reference standard (Rockville, MD).

2.2. Oligosaccharide analysis

2.2.1. Sugar analysis

For the determination of glucosamine (GlcN) content, COS hydrolysis was performed by addition of 1 mL of HCl 1 M to 1–2 mg of sample, followed by incubation at 100 °C for 24 h. In the case of the neutral sugars, the hydrolysis consisted in the addition of 0.5 mL of TFA 2 M and incubation at 120 °C for 1 h followed by evaporation of the TFA in a speedvac. After both hydrolysis, 2-deoxyglucose (1 mg/mL) was added as internal standard. The samples were then neutralized with 25% NH_3 and reduced by the addition of 100 µL of a $NaBH_4$ 15% (w/v) solution prepared in NH_3 3 M. After incubation at 30 °C for 1 h, 50 µL of glacial acetic acid were added two times to eliminate the BH_4^- in excess. The acetylation was carried by addition of acetic anhydride, using methyl imidazole as catalyst. The alditol acetates were extracted with dichloromethane and the solvent was evaporated using a speedvac. The derivatized sugars were dissolved in anhydrous acetone and then analysed by gas chromatography with a mass spectrometry detector (GC–MS, Shimadzu GCMS-QP2010 Ultra), as described elsewhere [24], using a HT-5 column (30 m long, 0.25 mm diameter, 0.10 µm film thickness). The temperature of the injector and detector were 350 °C and 250 °C, respectively. The oven initial temperature was 140 °C and reached a temperature of 180 °C for 1 min with a rate of 5 °C/min, followed by an increase at 5 °C/min until 250 °C and a second increase at a rate of 100 °C/min until 350 °C. The samples were analysed in triplicate and the sugars were identified based on their retention time and mass spectra.

2.2.2. Methylation analysis

Glycosidic linkages were determined after derivatization to partially methylated alditol acetates by GC–MS [25]. Briefly, the polysaccharides were methylated before hydrolysis, reduction, and acetylation to obtain partially methylated alditol acetates (PMAA). PMAA were injected in a GC–MS (Shimadzu GCMS-QP2010 Ultra) equipped with a HT-5 column (30 m long, 0.25 mm diameter, 0.10 μm film thickness). Helium was the carrier gas and had a flow rate of 1.84 mL/min. The temperature of the injector and detector was 250 °C. The initial temperature of the oven was 80 °C, followed by an increase of 7.5 °C/min until it reached 140 °C, which was maintained for 5 min, and a second increase of 15 °C/min until it reached 250 °C which was kept for 5 min. PMAA residues were identified based on their retentions time and mass spectra.

2.2.3. Deacetylation degree

The degree of deacetylation of the commercial water-soluble chitosan (COS) was confirmed using proton NMR methodology [26].

2.2.4. Size exclusion chromatography

About 5 mg of chitooligosaccharide sample was dissolved in 50 μL of 8% LiCl dimethylacetamide (DMA) solution at 80 °C for 4 h. The sample was then diluted in 2 mL of DMA and injected at 70 °C using an autosampler. The size exclusion chromatography (*SEC*) analysis was performed using Agilent PL-GPC 220 system (Agilent Technologies) equipped with two columns Agilent PL gel MIXED-D 7.5 × 300 mm, 5 μm in series protected by an Agilent PL gel MIXED precolumn, 7.5 × 50 mm, 5 μm. The columns, injector system, and the detector (RI) were maintained at 70 °C during the analysis. The eluent (0.5% w/v LiCl in dimethylformamide) was pumped at a flow rate of 0.9 mL/min. The columns were calibrated within the molecular weight range of 0.7–300.0 kDa using pullulan standards (Polymer Laboratories, Shropshire, UK).

2.3. In vitro cholesterol solubility assays using ^{13}C and ^{1}H solution NMR

In order to assess the potential of COS in the decrease of cholesterol solubility, mixtures of the COS with GDCA were added to [4-^{13}C] cholesterol films using the methodology described elsewhere, which has been previously used to follow the emulsification of cholesterol in the presence of phytosterols, tocopherol, saturated and unsaturated fatty acids, and polysaccharides [6,9,27]. Solutions of chitooligosaccharides and BS were individually prepared by solubilization in the buffer during 2 h and mixed together (equal volumes) during at least 3 h to obtain final concentration of 5 mg/mL and 50 mM, respectively. Because, upon mixing a white precipitate is formed, the samples were centrifuged, and the resultant supernatant was equilibrated with cholesterol film during 24 h to attain equilibrium.

The model used considered only a BS, glycodeoxycholic acid, which is one of the main BS present in intestinal lumen, at physiological concentrations (50 and 25 mM), and cholesterol 3.5 mM, representing an average 540 mg of cholesterol daily intake in 400 mL intestinal volume content, in buffered solutions at pH 7.4 and at 37 °C, in presence (150 mM) and absence of NaCl. Under these circumstances, the simplified *in vitro* intestinal model is suitable to disclose the possible mechanisms that may be involved in the interaction of BS with COS that are able to produce an expected variation on cholesterol emulsification. The buffer solutions used in solubility experiments were Tris-HCl 10 mM with pH 7.4 and 6.4, containing EDTA 1 mM, NaN_3 0.1%, and NaCl (150 and 0 mM) which were prepared in water, lyophilized, and reconstituted in deuterated water for NMR locking purposes.

^{13}C NMR with proton decoupling were acquired on a Bruker 500 MHz NMR spectrometer using a high field "switchable'' broadband 5 mm probe with z-gradient, operating at the frequency of 500.13 MHz (^{1}H spectra) and 125.8 MHz (^{13}C spectra). The working conditions for acquiring ^{13}C NMR spectra were a temperature of 37 °C, a pulse angle of 30 °, spectral width of 25,252 Hz with an acquisition time of 1.3 s, a relaxation delay of 5 s and 2048 scans. ^{1}H decoupling was addressed using a WALTZ-16 decoupling sequence. Nuclear Overhauser Enhancement (NOE) between ^{13}C-{^{1}H} was obtained by comparing ^{13}C spectra with full proton decoupling and ^{13}C spectra with proton decoupling only during spectral acquisition. ^{1}H NMR spectra were obtained at 37 °C, with a 90° pulse angle, a spectral width of 7500 Hz, acquisition time of 1.0 s, a relaxation delay of 5 s and 128 acquisition scans. Spectra were processed with MestreNova 6.1.1 (Mestrelab Research, Santiago de Compostela, Spain).

2.4. Electrophoretic mobility

The electrophoretic mobility of the COS solution (0.5 and 5 mg/mL), in absence and presence of glycodeoxycholic acid (GDCA) BS (0–50 mM), prepared in distilled water and buffered solutions (Tris pH 7.4 and 6.4) was measured using a Malvern Zetasizer Nano ZSP apparatus with pH adjustment using NaOH and HCl solutions (typically, 10 mM). Two types of experiments were addressed, one where the dependence of electrophoretic mobility of chitosan solutions at different pH was evaluated and another where the change of electrophoretic mobility was followed due to the interaction between BS and oligosaccharides. COS and GDCA were dissolved in water or buffer solutions with adjusted pH. For the measurements, a volume of 500 μL of each solution were mixed, giving rise to a white precipitate which was centrifuged (5 min, 13,793 *g*). The supernatant was transferred to the zeta potential cell and measured.

2.5. Statistical analysis

Results were expressed as the mean ± standard deviation. Statistical significance was determined using analysis of variance (ANOVA) and Tukey's test with $\alpha = 0.05$, using the Excel software (Microsoft, Seattle, WA, America).

3. Results and discussion

3.1. Chitooligosaccharides chemical analysis

The COS sample used in this work was composed only by glucosamine residues, with a ratio of (1 → 4)-GlcN to *t*-GlcN near 9 (Figure S1, provided as supplementary material). Accordingly, the average molecular weight was 1941 Da, determined by size exclusion chromatography (Figure S2, provided as supplementary material), and the degree of deacetylation of 90 % was obtained by ^{1}H NMR.

3.2. Effect of chitooligosaccharides on bile salt sequestration and cholesterol accessibility

The effect of COS in the sequestration of the BS glycodeoxycholic acid (GDCA) and on the lowering of cholesterol accessibility was evaluated by quantitative solution ^{13}C NMR, using different conditions able to approximate the fasted and fed state physiological conditions, [28] considering 50 and 25 mM concentration of GDCA. Moreover, different pH values (6.4 and 7.4), and ionic strength (0 and 150 mM NaCl), were tested to evaluate the relevance of ionic and non-ionic interactions on the sequestration of BS by COS, as well as on cholesterol bioaccessibility. Fig. 1 shows the superposition of solution ^{13}C NMR spectra obtained using the *in vitro* intestinal model composed of GDCA 50 mM (red line), GDCA 50 mM and ^{13}C labelled cholesterol 3.5 mM in the absence (orange line) and presence of COS 5 mg/mL (blue line) and colestipol 5 mg/mL (green line) in a buffered solution with Tris 10 mM at pH 7.4 in the presence of 150 mM of NaCl. Solution NMR only allows to detect signal from molecules in small aggregates. Therefore, only cholesterol solubilized in BS micelles is observed, without the contribution of precipitated cholesterol. Other large aggregates, such as COS with GDCA BS bounded are also not detected. This is because large aggregates have a slow

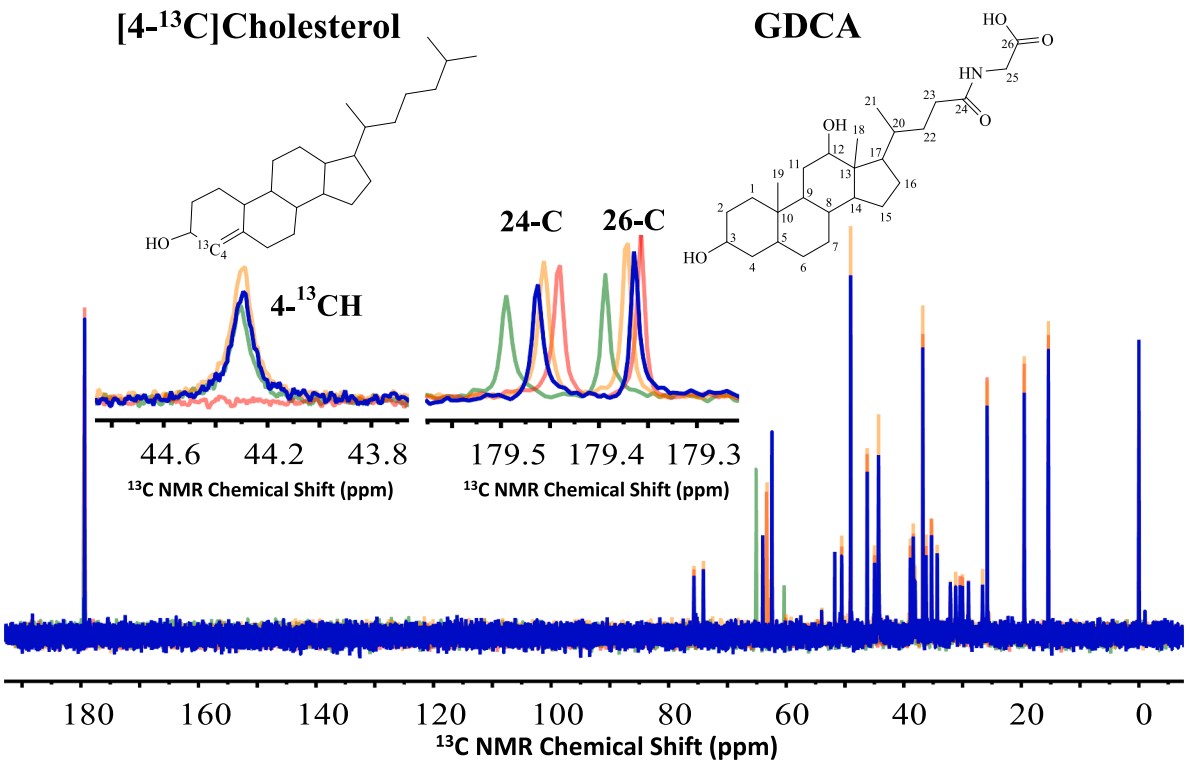

Fig. 1. Solution ^{13}C NMR spectra of BS glycodeoxycholic acid (GDCA 50 mM, red line) and GDCA 50 mM with [4-^{13}C]Cholesterol 3.5 mM (pH 7.4) in absence (orange line) and presence of COS 2.6 mM (5 mg/mL) (blue line) or cationic resin colestipol 5 mg/mL (green line). The insert highlights the decrease of the signals of cholesterol (Carbon 4 at 44.3 ppm) and GDCA (Carbon 24 and 26, at 179.5 and 179.4 ppm, respectively) in the presence of the COS and colestipol, reflecting the decrease in cholesterol accessibility and GDCA sequestration, respectively. (For interpretation of the references to colour in this figure legend, the reader is referred to the web version of this article.)

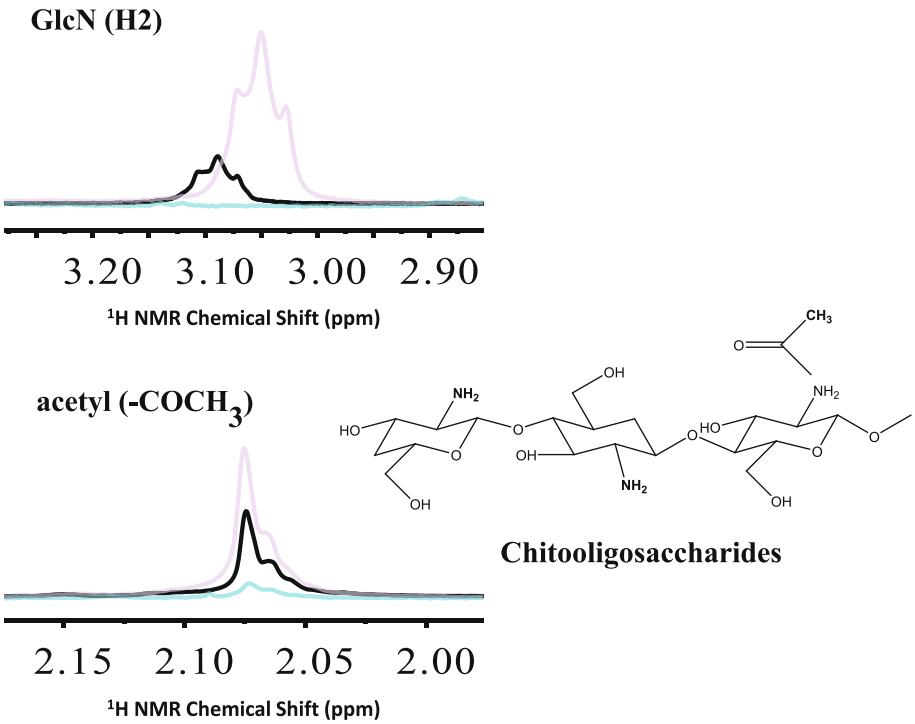

Fig. 2. Partial ^{1}H NMR spectra of COS 5 mg/mL (black line), GDCA 0.1 mM with chitooligosaccharide 5 mg/mL (pink line) and GDCA 50 mM with COS 5 mg/mL (cyan line), in Tris-HCl buffer in D_2O (pH 7.4). Relevant chemical shifts from chitooligosaccharide are highlighted. (For interpretation of the references to colour in this figure legend, the reader is referred to the web version of this article.)

tumbling in solution leading to a faster relaxation of transverse magnetization (T_2) due to enhanced anisotropic spin interactions, generating peaks too broad to be detected in the spectral baseline. The insert graph in Fig. 1 shows the resonance of labelled cholesterol [4-^{13}C] cholesterol at 44.3 ppm and GDCA methyl resonance of 24-C and 26-C at around 179.4 ppm. The intensity of both resonances decreased in the presence of the COS. This effect was also observed in the presence of a cationic resin, colestipol, currently used as a pharmacological hypocholesterolemic agent.

The concentration of COS used is like the therapeutic dose of colestipol used per day (2 g), considering an intestinal lumen volume of 400 mL. In addition, this concentration also approaches the suggested daily intake of 3 g of chitosan recognized for the maintenance of cholesterol blood levels [29]. Both colestipol and COS BS sequestration was also assessed by quantitative ^{1}H NMR (Fig. 2). This allowed crosschecking the results obtained by quantitative ^{13}C NMR using the methyl protons linked to carbon 18 of GDCA resonance and TSP standard. Fig. 2 shows the superposition of the ^{1}H NMR spectra of selected resonances from COS (5 mg/mL, black line), in the presence of GDCA (0.1 mM, pink line and 50 mM, cyan line).

The overall ^{1}H NMR spectra as well as inserts of selected resonances are given in supplementary material section (Figure S3 to S5). One evidence of the interaction between COS and BS is shown by the changes noticed in ^{1}H NMR spectra for the resonances of the hydrogen atoms linked to carbon 2 of GlcN (2-CH) and GlcNAc residues (CH_3) from acetyl groups, with the resonances attributed according to literature [30,31]. It was observed that chitooligosaccharide resonances GlcN and acetyl (CH_3) have a different behavior depending on the concentration of the BS GDCA. For a concentration of 0.1 mM of GDCA (pink line), an increase of intensity on the 2-CH and CH_3 resonances was observed relatively to the COS (black line). In contrast, those resonances disappear in the presence of the high excess of GDCA (50 mM, cyan line). These results can be explained by the formation of soluble aggregates, which increase the solubility of the COS at low concentrations of GDCA (0.1 mM). However, at a higher concentration of GDCA (50 mM), the fact that those resonances are no longer visible in the NMR spectrum indicates their immobilization in large aggregates. Moreover, a shift to lower ppm as well as a resonance broadening was observed for 2-CH. A small shift was also observed for CH_3 of the acetyl group. The observed changes suggest an electrostatic interaction between the negatively charged carboxylate group of GDCA and the partially protonated amino group of the COS. The small shift in the acetyl group may also reflect hydrophobic interaction. Fig. 3 present a graphical representation of the variations in the chemical shift of the BS ^{13}C resonances due to the presence cholesterol and the polymers. This analysis was addressed to discriminate the BS resonances that are more involved in the interactions with COS or the cationic resin. In a previous work, a similar analysis showed that the carbons from the non-polar face of GDCA were the most affected, in agreement with hydrophobic interaction [27].

Considering the chemical nature of colestipol cationic resin, one of the expected interaction would be with the negatively charged carboxylic group and the nearby region. Indeed, this is observed in the Fig. 3, with the BS resonances C24 and C26 showing the larger shift. In contrast, the BS resonances that showed a larger shift with the presence of COS are mostly in the non-polar face of the BS (C7 and C15), sugesting non-ionic interactions. Although, hydrogen bonding cannot be discarded, no evidence was obtained from the chemical shift analysis of carbon resonances near the hydroxyl groups.

Aside from chemical shift analysis, ^{13}C NMR spectra allowed to determine the areas of cholesterol and GDCA signals and was used for their quantification. The dependence on the presence of COS and colestipol was evaluated and shown in Fig. 4.

The efficiency of COS and colestipol on the sequestration of BS at 50 mM, pH 7.4, and in the presence of NaCl 150 mM was 25% (blue bar) and 35% (green bar), respectively. This corresponds to 1.3 to 1.7 g of GDCA sequestered per g of polymer (Fig. 4A). Alongside, it was observed a similar decrease in the percentage of cholesterol emulsified in small aggregates (Fig. 4B). The proportionality observed between the amount of GDCA present in solution and that of solubilized cholesterol indicates that the lowering of cholesterol accessibility is due to the sequestration of BS by the polymers.

In order to approach the fasted physiological lumen conditions, a lower concentration of BS GDCA (25 mM, pH 7.4) was also studied in the presence of COS 5 mg/mL, showing a sequestration of 1.1 g per g of polymer (Fig. 4A). The influence of ionic strength was also studied regarding the BS sequestration and cholesterol solubility at pH 7.4 and 6.4. In absence of COS at pH 7.4, the presence of NaCl leads to an increase on the solubility of cholesterol (Fig. 4 B, orange and salmon

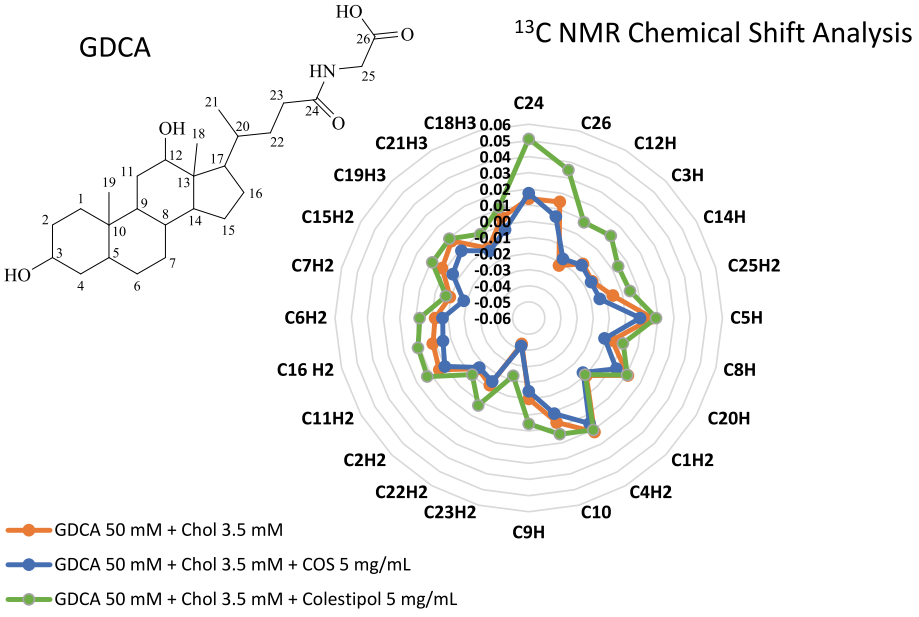

Fig. 3. ^{13}C Chemical shift analysis of BS resonances in the presence of cholesterol (orange line), and additionally COS (blue line) or Colestipol (green line). The resonances of GDCA (C17 and C13) were not used in the chemical shift analysis, due to their partial overlap. (For interpretation of the references to colour in this figure legend, the reader is referred to the web version of this article.)

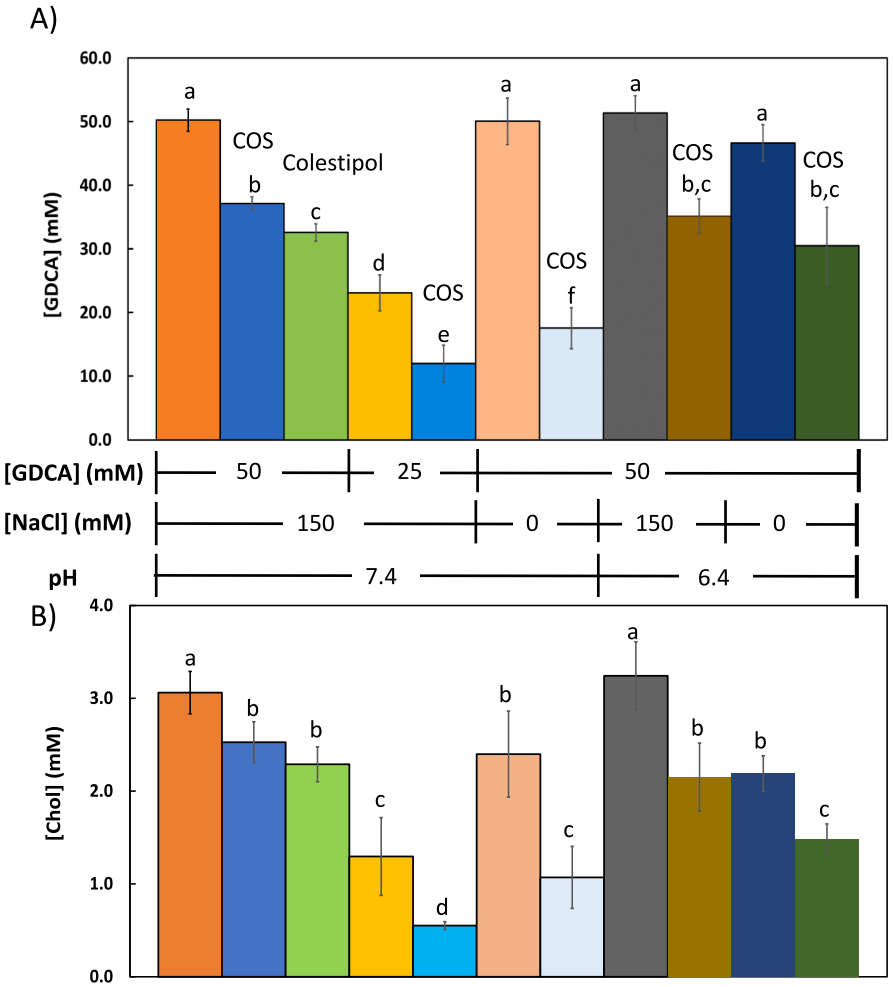

Fig. 4. Effect of COS in the different conditions described in the legend (**A**) Sequestration of BS by the COS at a concentration 5 mg/ mL; (**B**) Decrease of cholesterol solubilized in the presence of COS in a simplified *in vitro* intestinal model composed by GDCA and [4-^{13}C]cholesterol. Different letters indicate significant statistical difference between groups with $\alpha = 0.05$.

colour bar). This is possibly due to the decrease of charge repulsion between BS in the micelles, similarly to what has been described for SDS micelles [32]. In the same conditions, the presence of COS leads to an increase in BS sequestration as well as a decrease in the solubility of cholesterol, showing a resemblant dependence on the presence of NaCl. The change of pH from 7.4 to 6.4 did not show statistically significant difference in the BS sequestration and cholesterol solubility, both in the presence and absence of COS. These results show that COS sequestration and cholesterol emulsification are not affected by the pH range (6.4–7.4) variations during their transit in the intestinal tract. However, it would be expected that a decrease in the pH could lead to an increase in the charge character of the COS, affecting the sequestration of BS. To further elucidate on the importance of electrostatic interactions between COS and GDCA, the electrophoretic mobility of the polymer was characterized as a function of pH.

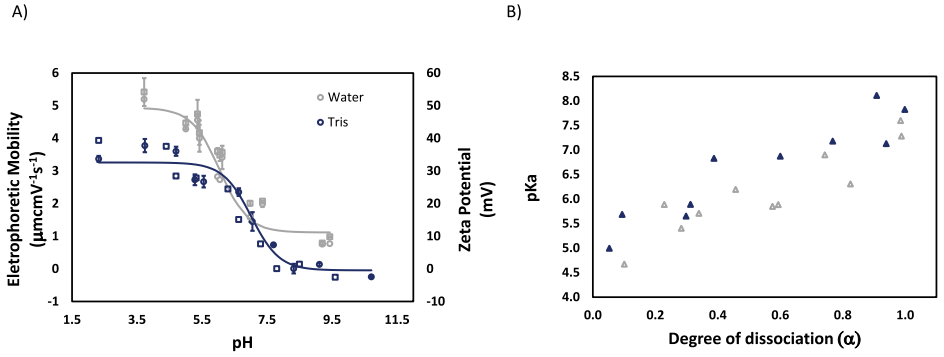

Fig. 5. A) Dependence of the electrophoretic mobility (circles) and zeta potential (squares) of water-soluble COS with the pH in water and Tris buffer (The line represents the best fit of the data set using the Henderson-Hasselbalch equation). B) Variation of pKa in function of the degree of dissociation.

3.3. Characterization of chitooligosaccharides pKa and bile salts-chitooligosaccharides electrophoretic mobility and size

Electrophoretic mobility measurements were performed for COS at a concentration of 0.5 mg/mL and different pH values (typically 4–10) to determine its ionization constant (Fig. 5A), using water and Tris buffer (10 mM). The zeta potential, which derives from electrophoretic mobility measurements, was 45 mV in aqueous medium at pH 4.0, where the amino groups of GlcN residues were protonated, and decreased with the increase of pH, with a strong variation between pH 5 and 8, from 42 to 10 mV. This high variation of zeta potential with the pH allowed to estimate a pKa of 6.0 for the COS under study, similar to 6.2 to 6.5 values reported in the literature [16]. The positive zeta potential at all pH range studied shows that the COS still have positive charge in water. At physiological pH (7.4) the zeta potential is 14 mV. This is in accordance with the zeta potential value of 4 mV of a low molecular weight chitooligosaccharide reported [33]. These results may be explained by COS binding capacity for metal ions, both negative and positive, described for chitosan [34].

The pH dependence was also analyzed in the presence of Tris buffer showing a higher pKa (7.0) for COS. In Fig. 5A, it may be seen that the best fit assuming a single ionization constant does not fully describe the point data set, with systematic deviations at the extreme pH values. This suggests that the pKa varies with the degree of ionization. The electrophoretic mobility (μ) dependence on pH was used to determine the dissociation degree (α) as described in SI (section 1) and is shown in Fig. 5B. In fact, it is observed an increase in pKa (from 5 to 8) with the increase of COS degree of dissociation. This is a typical behavior of charged polymers, with a destabilization of the charged form at higher charge density and have been previously observed for COS [35]. In agreement with the best fit obtained considering a single pKa value (Fig. 5A), the apparent pKa obtained in Tris tends to be higher than that obtained in water (Fig. 5B). This suggests that some of the ions present in the Tris buffer solution may be interacting with COS, stabilizing the ionized (non-dissociated) species. This agrees with the observation that the charge density obtained in this solvent at full COS ionization is smaller than the value obtained in water.

An interaction of the negatively charged GDCA (pKa of 4.8 [1]) with COS positively charged glucosamine residues will decrease the polymer charge density, and is expected to lead to an increase in the apparent pKa of the free glucosamine residues. At high BS content the charge density of COS-BS complex will decrease and the apparent pKa will approach 8. Both pH́s (6.4 and 7.4) studied are well below this pKa and therefore all glucosamine residues may be ionized. This may partially explain the similar results obtained at both pH values regarding the binding of BS and the decrease in cholesterol bioaccessibility (Fig. 3).

In order to further investigate these interactions, aqueous solutions of COS (5 mg/mL, 2.6 mM considering the average molecular weight 1990 Da, Figure S2) with different GDCA concentrations (0 to 50 mM) were used to measure the changes in their electrophoretic mobility and size, at different buffer pH solutions (Fig. 6 A and B).

The titration of chitooligosaccharide with BS leads to the formation of a white precipitate, which increased with the concentration BS (SI, Figure S7). The precipitate is only visibly evident at BS concentrations above 5 mM, suggesting that no precipitation occurs at lower concentrations. After centrifugation, the electrophoretic mobility and size of the supernatant was characterized. At low concentrations of BS (<15 mM) only a small decrease in the electrophoretic mobility is observed. For higher concentrations an abrupt variation occurs, attaining negative electrophoretic mobility values. The exact value where this variation occurs depends on the solvent, being higher for Tris pH 6.4 (30 to 40 mM of GDCA) and lower for water (20 to 25 mM of GDCA), as shown in Fig. 6A and SI (Figure S6).

The size of aggregates in solution is shown in Fig. 6B. It is observed that the diameter is larger than 150 nm and increases abruptly after the transition from positive to negative electrophoretic mobility. The characteristic size of those samples were much higher than the average size of BS micelles which is reported to be of 2 nm of diameter, in 150 mM NaCl [6]. A decrease in ionic strength is expected to decrease the aggregation number of BS micelles as well as critical micellar concentration [1]. Therefore, at the conditions used in this experimental setting, the BS micelles size is expected to be smaller. This highlights that the large aggregates in solution, should be composed by complexes of COS and BS.

The supernatants were analyzed by ^{1}H NMR to quantify the amount of BS at both pH́s (7.4 and 6.4). No signal from BS was observed within 1.25 mM and 20 mM, highlighting that in this concentration range all the BS are in large aggregates or have been precipitated with COS. At higher concentrations it was possible to determine BS content, being 14 ± 2 and 24 ± 2 for 50 mM of GDCA, at pH 7.4 and 6.4, respectively. The amount of BS sequestered by COS agrees with the results obtained in the solubility assays in the absence NaCl (see Fig. 4A, light blue and green olive colour bar). Fig. 7 shows the dependence of the amount of BS in small aggregates (measured by ^{1}H NMR) with total BS concentration.

As indicated before, bellow 20 mM of GDCA, no BS was detected in solution. Above this concentration there is a linear increase showing the

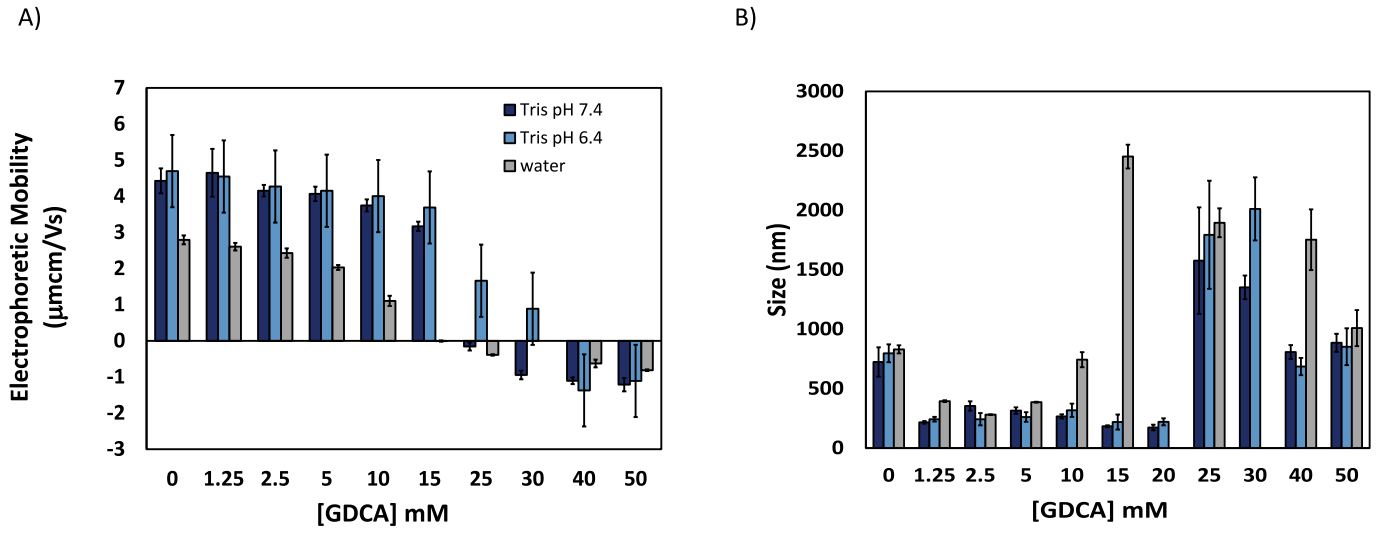

Fig. 6. A) Dependence of the measured electrophoretic mobility of COS in the presence of increasing concentrations of GDCA considering different solvents. B) Size of the COS-BS aggregates in suspension for the different conditions tested. The standard deviation is from at least 3 independent experiments.

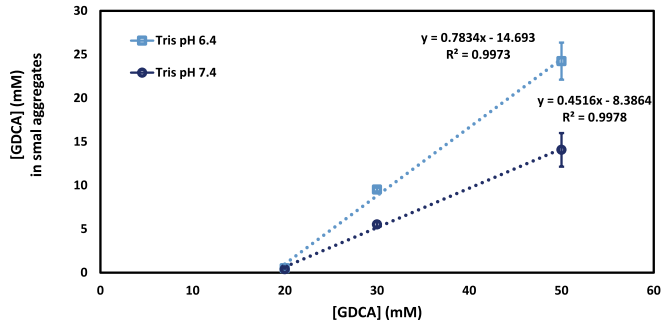

Fig. 7. Amount of BS in small aggregates as a function of total BS concentration. The standard deviation is from at least 3 independent experiments.

presence of excess of BS in small aggregates. However, the slope is smaller than one, highlighting that some of the added BS is binding to COS to form large aggregates (Fig. 6B). From Fig. 6A it is observed that this is occurring even after the attainment of neutral electrophoretic mobility.

It has been described that BS can form supramolecular helices upon the interaction with oppositely charged polyelectrolytes [13] and also that their interaction with oppositely charged polymers, can lead to different supramolecular morphologies such as globular and tape-like [12]. It is conceivable that in the present system a similar supramolecular aggregate can be formed which may impact on BS emulsifying effect on lipids and lipophilic compounds, particularly at the intestinal lumen pH 6.4 but also in the enterohepatic recirculation of BS at ileum which has a higher pH 7.4.

4. Conclusions

In this work, the mechanism for the decrease in cholesterol bioaccessibility by a water-soluble COS (average degree of polymerization of 10 and 90 % deacetylation degree) was studied.

In vitro cholesterol solubility assays showed that the COS were effective in the decrease of cholesterol accessibility, both at pH 7.4 and 6.4. In these conditions, chitooligosaccharides showed a similar BS sequestration capacity, being resemblant to the cationic resin colestipol, demonstrating their potential for affecting cholesterol bioaccessibility.

The results obtained show that COS is able to sequester BS due to both ionic and non-ionic interactions. Evidence for the expected ionic interactions were obtained by i) ^{1}H NMR (chemical shift analysis) with a substantial shift of COS glucosamine in the presence of GDCA (Fig. 2); and ii) the effect of ionic strength, with a higher bile salt sequestration efficiency at lower ionic strength. In addition, strong evidence was obtained regarding the involvement of non-ionic interactions, namely i) a small shift was observed in acetylated glucosamine by the presence of BS; ii) the electrophoretic mobility of GDCA-COS aggregates at high GDCA concentrations becomes negative; and iii) a similar effect on sequestration of BS was observed for both pH's.

The COS concentration of 5 mg/mL used in this work was very efficient in the sequestration of GDCA up to 20 mM, and at higher GDCA concentrations a significant sequestration still occurs. When the total concentration of BS is 25 mM, about 50% is sequestered corresponding to 1.1 g of BS per g of COS. While a total concentration of 50 mM, 25 % of BS is sequestered corresponding to 1.3 g per g of COS. Therefore, COS is more efficient for physiological conditions where BS concentrations are lower than 25 mM. When the ionic strength is decreased an increase in the amount of BS sequestered is observed corresponding to 3.2 g per g of COS at a total GDCA concentration of 50 mM. Considering the molecular weight of GDCA and each glucosamine residue this corresponds to about 2 glucosamines per BS at 150 mM of NaCl and 1 glucosamine per BS a low ionic strength. If the ionization of glucosamine residues (50 % at pH 6.4 and 10 % ionized at pH 7.4) is taken in account, the ratio of BS per ionized glucosamine is 1 at pH 6.4 and increases to 4 at pH 7.4. This highlights that while at pH 6.4 the ionic interactions may predominate, a strong contribution from additional interactions (such as hydrogen bonding and hydrophobic interactions) is observed at pH 7.4.

This work highlights that the interaction between COS and BS, at physiological pH, commonly attributed to electrostatic interactions, has also a contribution of the hydrophobic character of both components. The understanding of the contribution of these non-ionic interactions is a relevant feature which can aid in the development of hydrophilic hypocholesterolemic agents based on carbohydrates.

Funding

This research was funded by Fundação para a Ciência e a Tecnologia (FCT)/MCTES for the support to the research units QOPNA (FCT UID/QUI/00062/2019), LAQV-REQUIMTE (UIDB/50006/2020 & UIDP/50006/2020), CICECO (UIDB/50011/2020; UIDP/50011/2020 & LA/P/0006/2020) and CQC (UIDB/00313/2020 & UIDP/00313/2020); and also supported by the projects PTDC/QUI-OUT/29373/2017 and POCI 01-0145-FEDER-031032, through national funds (OE) and where applicable co-financed by the FEDER, by the Operational Program of Competitiveness and Internationalization (POCI), within the PT2020 Partnership Agreement. I.M.V.S and F.M.C.G. were supported by master fellow and research contract framed on PTDC/QUI-OUT/29373/2017 and LAQV-REQUIMTE (UIDB/50006/2020) projects. C.N. was funded by national funds (OE), through FCT, I.P., within the scope of the framework contract foreseen in the numbers 4, 5 and 6 of the article 23, of the Decree-Law 57/2016, of August 29, changed by Law 57/2017, of July 19.

CRediT authorship contribution statement

Filipe Coreta-Gomes: Conceptualization, Formal analysis, Funding acquisition, Investigation, Methodology, Supervision, Writing – original draft, Writing – review & editing. **Inês M.V. Silva:** Investigation, Writing – original draft. **Cláudia Nunes:** Conceptualization, Investigation, Writing – original draft, Writing – review & editing. **Ildefonso Marin-Montesinos:** Writing – review & editing. **Dmitry Evtuguin:** Formal analysis, Investigation.**Carlos F.G.C. Geraldes:** Writing – review & editing. **Maria João Moreno:** Formal analysis, Conceptualization, Methodology, Writing – review & editing. **Manuel A. Coimbra:** Conceptualization, Formal analysis, Writing – review & editing.

Declaration of Competing Interest

The authors declare that they have no known competing financial interests or personal relationships that could have appeared to influence the work reported in this paper.

Data availability

Data will be made available on request.

Appendix A. Supplementary data

Supplementary data to this article can be found online at https://doi.org/10.1016/j.jcis.2023.05.056.

References

[1] M.C. Carey, Micelle Formation by Bile Salts, Arch. Intern. Med. 130 (1972) 506, https://doi.org/10.1001/archinte.1972.03650040040005.
[2] O. Pabois, C.D. Lorenz, R.D. Harvey, I. Grillo, M.M.L. Grundy, P.J. Wilde, Y. Gerelli, C.A. Dreiss, Molecular insights into the behaviour of bile salts at interfaces: a key to their role in lipid digestion, J. Colloid Interface Sci. 556 (2019), https://doi.org/10.1016/j.jcis.2019.08.010.
[3] O. Hernell, J.E. Staggers, M.C. Carey, Physical-chemical behavior of dietary and biliary lipids during intestinal digestion and absorption. 2. Phase analysis and aggregation states of luminal lipids during duodenal fat digestion in healthy adult

human beings, Biochemistry. 29 (1990) 2041–2056, https://doi.org/10.1021/bi00460a012.
[4] J.E. Staggers, O. Hernell, R.J. Stafford, M.C. Carey, Physical-chemical behavior of dietary and biliary lipids during intestinal digestion and absorption. 1. Phase behavior and aggregation states of model lipid systems patterned after aqueous duodenal contents of healthy adult human beings, Biochemistry. 29 (1990) 2028–2040, https://doi.org/10.1021/bi00460a011.
[5] I.M.V. Silva, F. Machado, M.J. Moreno, C. Nunes, M.A. Coimbra, F. Coreta-Gomes, Polysaccharide structures and their hypocholesterolemic potential, Molecules. 26 (2021) 4559, https://doi.org/10.3390/molecules26154559.
[6] F.M. Coreta-Gomes, W.L.C.C. Vaz, E. Wasielewski, C.F.G.G. Geraldes, M.J. Moreno, Quantification of cholesterol solubilized in dietary micelles: Dependence on human bile salt variability and the presence of dietary food ingredients, Langmuir. 32 (2016) 4564–4574, https://doi.org/10.1021/acs.langmuir.6b00723.
[7] M.D. Siperstein, I.L. Chaikoff, W.O. Reinhardt, C14-Cholesterol. V., Obligatory function of bile in intestinal absorption of cholesterol, J. Biol. Chem. 198 (1952) 111–114. http://www.ncbi.nlm.nih.gov/pubmed/12999722.
[8] O. Pabois, R.M. Ziolek, C.D. Lorenz, S. Prévost, N. Mahmoudi, M.W.A. Skoda, R.J. L. Welbourn, M. Valero, R.D. Harvey, M.M.L. Grundy, P.J. Wilde, I. Grillo, Y. Gerelli, C.A. Dreiss, Morphology of bile salts micelles and mixed micelles with lipolysis products, from scattering techniques and atomistic simulations, J. Colloid Interface Sci. 587 (2021) 522–537, https://doi.org/10.1016/j.jcis.2020.10.101.
[9] F.M. Coreta-Gomes, G.R. Lopes, C.P. Passos, I.M. Vaz, F. Machado, C.F.G. C. Geraldes, M.J. Moreno, L. Nyström, M.A. Coimbra, In vitro hypocholesterolemic effect of coffee compounds, Nutrients. 12 (2020) 437, https://doi.org/10.3390/nu12020437.
[10] A.S.P. Moreira, D. Gaspar, S.S. Ferreira, A. Correia, M. Vilanova, M.-M. Perrineau, P.D. Kerrison, C.M.M. Gachon, M.R. Domingues, M.A. Coimbra, F.M. Coreta-Gomes, C. Nunes, Water-Soluble Saccharina latissima Polysaccharides and Relation of Their Structural Characteristics with In Vitro Immunostimulatory and Hypocholesterolemic Activities, Mar. Drugs. 21 (2023), https://doi.org/10.3390/md21030183.
[11] C.L. Pires, I.M.V. Silva, M.A. Coimbra, M.J. Moreno, F. Coreta-Gomes, Effect of Coffee on the Bioavailability of Sterols, Foods. 11 (2022) 2935, https://doi.org/10.3390/foods11192935.
[12] K. Schillén, L. Galantini, G. Du, A. Del Giudice, V. Alfredsson, A.M. Carnerup, N. V. Pavel, G. Masci, B. Nyström, Block copolymers as bile salt sequestrants: Intriguing structures formed in a mixture of an oppositely charged amphiphilic block copolymer and bile salt, Phys. Chem. Chem. Phys. 21 (2019) 12518–12529, https://doi.org/10.1039/c9cp01744e.
[13] G. Du, D. Belić, A. Del Giudice, V. Alfredsson, A.M. Carnerup, K. Zhu, B. Nyström, Y. Wang, L. Galantini, K. Schillén, Condensed Supramolecular Helices: The Twisted Sisters of DNA, Angew. Chemie - Int. Ed. 61 (2022), https://doi.org/10.1002/anie.202113279.
[14] M. Thongngam, D.J. McClements, Isothermal titration calorimetry study of the interactions between chitosan and a bile salt (sodium taurocholate), Food Hydrocoll. 19 (2005) 813–819, https://doi.org/10.1016/j.foodhyd.2004.11.001.
[15] S.P. Strand, T. Tømmeraas, K.M. Vårum, K. Østgaard, Electrophoretic light scattering studies of chitosans with different degrees of N-acetylation, Biomacromolecules. 2 (2001), https://doi.org/10.1021/bm015598x.
[16] Q.Z. Wang, X.G. Chen, N. Liu, S.X. Wang, C.S. Liu, X.H. Meng, C.G. Liu, Protonation constants of chitosan with different molecular weight and degree of deacetylation, Carbohydr. Polym. 65 (2006) 194–201, https://doi.org/10.1016/j.carbpol.2006.01.001.
[17] H. Pan, Q. Yang, G. Huang, C. Ding, P. Cao, L. Huang, T. Xiao, J. Guo, Z. Su, Hypolipidemic effects of chitosan and its derivatives in hyperlipidemic rats induced by a high-fat diet, Food Nutr. Res. 60 (2016) 31137, https://doi.org/10.3402/fnr.v60.31137.
[18] Y. Maezaki, K. Tsuji, Y. Nakagawa, Y. Kawai, M. Akimoto, T. Tsugita, W. Takekawa, A. Terada, H. Hara, T. Mitsuoka, Hypocholesterolemic Effect of Chitosan in Adult Males, Biosci. Biotechnol. Biochem. 57 (1993) 1439–1444, https://doi.org/10.1271/bbb.57.1439.
[19] J. Liu, J. Zhang, W. Xia, Hypocholesterolaemic effects of different chitosan samples in vitro and in vivo, Food Chem. 107 (2008) 419–425, https://doi.org/10.1016/j.foodchem.2007.08.044.
[20] W. Xu, A. Mohan, N.L. Pitts, C. Udenigwe, B. Mason, Bile acid-binding capacity of lobster shell-derived chitin, chitosan and chitooligosaccharides, Food Biosci. 33 (2020), 100476, https://doi.org/10.1016/j.fbio.2019.100476.
[21] P.V. Mendonça, M.J. Moreno, A.C. Serra, S. Simões, J.F.J. Coelho, Synthesis of tailor-made bile acid sequestrants by supplemental activator and reducing agent atom transfer radical polymerization, RSC Adv. 6 (2016) 52143–52153, https://doi.org/10.1039/C6RA06087K.
[22] M.M. Cassidy, F.G. Lightfoot, L.E. Grau, T. Roy, J.A. Story, D. Kritchevsky, G. V. Vahouny, Effect of bile salt-binding resins on the morphology of rat jejunum and colon - A scanning electron microscopy study, Dig. Dis. Sci. 25 (1980), https://doi.org/10.1007/BF01315212.
[23] H. Ko, M.E. Royer, In vitro binding of drugs to colestipol hydrochloride, J. Pharm. Sci. 63 (1974), https://doi.org/10.1002/jps.2600631218.
[24] G.R. Lopes, A.S. Ferreira, M. Pinto, C.P. Passos, E. Coelho, C. Rodrigues, C. Figueira, S.M. Rocha, F.M. Nunes, M.A. Coimbra, Carbohydrate content, dietary fibre and melanoidins: Composition of espresso from single-dose coffee capsules, Food Res. Int. 89 (2016) 989–996, https://doi.org/10.1016/j.foodres.2016.01.018.
[25] M.A. Coimbra, I. Delgadillo, K.W. Waldron, R.R. Selvendran, in: Isolation and Analysis of Cell Wall Polymers from Olive Pulp, Plant Cell Wall Anal., Springer, Berlin, Heidelberg, 1996, pp. 19–44, https://doi.org/10.1007/978-3-642-60989-3_2.
[26] M. Lavertu, Z. Xia, A.N. Serreqi, M. Berrada, A. Rodrigues, D. Wang, M. D. Buschmann, A. Gupta, A validated 1H NMR method for the determination of the degree of deacetylation of chitosan, J. Pharm. Biomed. Anal. 32 (2003) 1149–1158, https://doi.org/10.1016/S0731-7085(03)00155-9.
[27] F.M. Coreta-Gomes, W.L.C. Vaz, E. Wasielewski, C.F.G.C. Geraldes, M.J. Moreno, Quantification of cholesterol solubilized in bile salt micellar aqueous solutions using 13C nuclear magnetic resonance, Anal. Biochem. 427 (2012) 41–48, https://doi.org/10.1016/j.ab.2012.04.028.
[28] Z. Vinarov, M. Abdallah, J.A.G. Agundez, K. Allegaert, A.W. Basit, M. Braeckmans, J. Ceulemans, M. Corsetti, B.T. Griffin, M. Grimm, D. Keszthelyi, M. Koziolek, C. M. Madla, C. Matthys, L.E. McCoubrey, A. Mitra, C. Reppas, J. Stappaerts, N. Steenackers, N.L. Trevaskis, T. Vanuytsel, M. Vertzoni, W. Weitschies, C. Wilson, P. Augustijns, Impact of gastrointestinal tract variability on oral drug absorption and pharmacokinetics: An UNGAP review, Eur. J. Pharm. Sci. 162 (2021), https://doi.org/10.1016/j.ejps.2021.105812.
[29] M.J. Sadler, J. Funnell, Authorised EU health claim for chitosan, in: Foods, Nutr. Food Ingredients with Auth. EU Heal. Claims, Elsevier, 2018, pp. 161–178, https://doi.org/10.1016/B978-0-08-100922-2.00011-5.
[30] E. Fernandez-Megia, R. Novoa-Carballal, E. Quiñoá, R. Riguera, Optimal routine conditions for the determination of the degree of acetylation of chitosan by 1H-NMR, Carbohydr. Polym. 61 (2005) 155–161, https://doi.org/10.1016/j.carbpol.2005.04.006.
[31] Y. Yang, R. Xing, S. Liu, Y. Qin, K. Li, H. Yu, P. Li, Immunostimulatory Effects of Chitooligosaccharides on RAW 264.7 Mouse Macrophages via Regulation of the MAPK and PI3K/Akt Signaling Pathways, Mar. Drugs. 17 (2019) 36, https://doi.org/10.3390/md17010036.
[32] S. Pal, S.P. Moulik, Cholesterol solubility in mixed micellar solutions of ionic and non-ionic surfactants, J. Lipid Res. 24 (1983), https://doi.org/10.1016/s0022-2275(20)37878-0.
[33] S.H. Chang, H.T.V. Lin, G.J. Wu, G.J. Tsai, pH Effects on solubility, zeta potential, and correlation between antibacterial activity and molecular weight of chitosan, Carbohydr. Polym. 134 (2015), https://doi.org/10.1016/j.carbpol.2015.07.072.
[34] I.M.N. Vold, K.M. Vårum, E. Guibal, O. Smidsrød, Binding of ions to chitosan - Selectivity studies, Carbohydr. Polym. 54 (2003), https://doi.org/10.1016/j.carbpol.2003.07.001.
[35] M.W. Anthonsen, O. Smidsrød, Hydrogen ion titration of chitosans with varying degrees of N-acetylation by monitoring induced 1H-NMR chemical shifts, Carbohydr. Polym. 26 (1995), https://doi.org/10.1016/0144-8617(95)00010-5.